Received 13 February 2020; revised 14 March 2020; accepted 16 March 2020. Date of publication 23 March 2020; date of current version 13 April 2020.
Digital Object Identifier 10.1109/OJAP.2020.2982507

Analysis of Electromagnetic Energy Absorption in the Human Body for Mobile Terminals

HANYANG WANG (Senior Member, IEEE)
Department of Radio Performance Technology, Huawei Technologies (U.K.) Company Ltd., Reading RG2 6UF, U.K.
CORRESPONDING AUTHOR: H. WANG (e-mail: hanwanga@hotmail.com).

ABSTRACT The human body's absorption of electromagnetic fields from communication enabled devices has consistently been a research topic for both researchers from universities and companies in the mobile communication industry. The absorption of electromagnetic fields could mainly result in two consequences: (a) antenna radiation efficiency of the device could deteriorate dramatically; and (b) a large amount of the radiated power could be dissipated into the human body, such as the hand, ear, scalp and brain, which is defined and described by Specific Absorption Rate (SAR). A comprehensive analysis of electromagnetic field absorption by the human body has been carried out to explain and answer some of the key questions in this area.

INDEX TERMS Handset antennas, RF exposure, specific absorption rate (SAR), antenna radiation efficiency.

I. INTRODUCTION

COMMUNICATION enabled devices, such as smart phones and smart watches, have been widely used in our daily life. The interaction and absorption of electromagnetic fields with the human body have received considerable attention over the past many years. A measure of this absorbed electromagnetic power by the human body is known as Specific Absorption Rate (SAR). There are currently two different standards worldwide. The SAR specified by FCC is that the maximum allowed power deposition is 1.6 W/kg in 1g of tissue from exposure to a communication enabled device (U.S. and Canada), whereas the International Commission on Non-Ionizing Radiation Protection (ICNIRP) requires a maximum allowed power deposition of 2 W/kg in any 10g of tissue (EU, China, Japan and Brazil).

Significant work and progress have been reported in recent years to develop more accurate methods of SAR evaluation and measurements and SAR reduction techniques for mobile hand-held and wearable devices [1]–[6]. However, most of the reported work has been focused on practical approaches, rather than theoretical methodology, to design antennas of mobile devices with low SAR values, and many key questions associated with SAR remain unanswered. Based on the SAR definition, the SAR value should be given by

$$\mathbf{SAR} = \sigma \mathbf{E^2}/\rho \tag{1}$$

where σ is the conductivity of the human body [S/m]; E is the induced electric field inside the human body [V/m]; and ρ is the density of the human body [kg/m^3]. The unit of SAR value is therefore W/kg. For standing wave antennas used in most mobile devices, such as Planar Inverted-F Antennas (PIFA) and monopole antennas, the maximum electric field and the magnetic field are at different locations. Just like a standing wave in a transmission line, the location of the maximum electric field in these antennas is actually the location of the minimum magnetic field, and vice versa. In SAR simulations and measurements for the antenna design of mobile devices, the maximum hotspots of simulated and measured SAR in a human body always correspond to the highest electric current area of the antenna or the printed circuit board (PCB), which is proportional to the tangential component of the magnetic field. This phenomenon was actually observed in 1990s when SAR was studied using dipole antennas [7]–[8]. However, according to the SAR definition as given by equation (1), the SAR value is proportional to the electric strength in the human body and the absorption is caused by the electric field. This is why SAR measurement systems for mobile devices, such as the well-known DASY system, use electric field probes for SAR measurements. This "contradiction" has puzzled many researchers and engineers working in this area for many years. To the author's knowledge, there are no published research papers

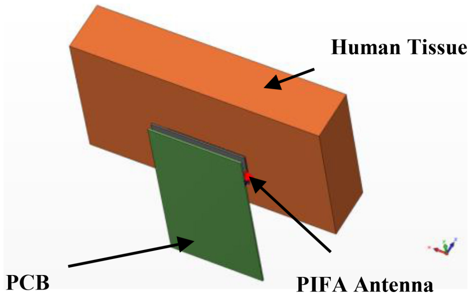

FIGURE 1. A mobile device being closely placed to the human tissue.

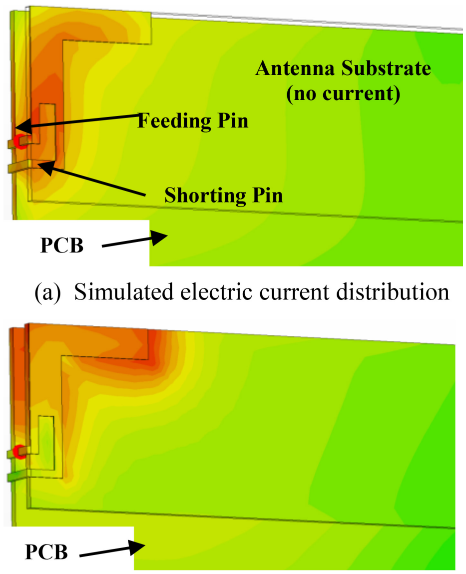

(a) Simulated electric current distribution

(b) Simulated electric field distribution

FIGURE 2. Simulated results of PIFA antenna.

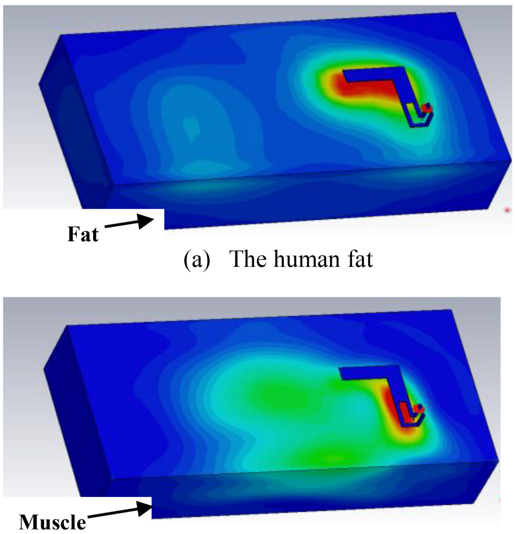

(a) The human fat

(b) The human muscle

FIGURE 3. Simulated electromagnetic power absorption.

or other publications in the literature to comprehensively explain this phenomenon. Unless this puzzle is solved, it is very difficult to understand the mechanism of electromagnetic field absorption in the human body so as to find accurate and effective approaches for SAR reduction.

It is the purpose of this paper to study and analyze the mechanism of electromagnetic field absorption in the human body in the antenna design of mobile devices and to explain and solve this puzzle. The analysis is based on the boundary conditions of electromagnetic fields at the interfaces of the antenna and/or PCB, air gap and the human tissue that could be fat, muscle, skin or combination of them, in which a mobile device with an antenna is closely placed to the human body. Simulated results for simplified models at a typical frequency for mobile devices are initially presented to demonstrate how the electromagnetic field interacts with and penetrates the human body. More realistic models with a whole human phantom head has been subsequently simulated and analysed. Based on these results the phenomenon outlined above can be easily explained and understood.

II. ELECTROMAGNETIC FIELD ABSORPTION

Fig. 1 (a) shows an antenna mounted on a PCB of a mobile device and a block of dielectric material representing the human tissue. The antenna is designed to operate at the frequency band from 1710 to 2170 MHz. The simulated electric current and the electric field at frequency 1850 MHz are given in Fig. 2. As can be observed, the electric current and electric field distributions are indeed the same as described in the previous section, namely the maximum location of the electric current being the minimum location of the electric field, and vice versa.

The simulated electromagnetic power absorption in the block of the human tissue is illustrated in Fig. 3. Two cases have been examined: in the first case the human tissue is the fat with dielectric constant = 4.9, conductivity = 0.03 S/M and the density 1100 kg/m^3, while in the second case the human tissue is the muscle with dielectric constant = 54.0, conductivity = 1.0 S/M and the density 1050 kg/m^3. The spacing between the top surface of the PIFA antenna and the block of the human tissue is 4.0 mm in these simulations. The frequency used in the simulation is 1800 MHz. It can be seen that for the first case, the location of the hotspot is close to the open end of the PIFA antenna that is the maximum electric field area. This is in agreement with the SAR definition described by equation (1). On the other hand, for the human muscle case, the SAR hotspot is located at the feeding area of the PIFA antenna where the electric current reaches its peak value. Other spacings, such as 2.0 mm or 6.0 mm, have also been simulated, and the results are very similar to those with the 4.0 mm spacing. As mentioned in the previous section, the phenomenon in the second case has been observed and experienced by many researchers and engineers who are working in SAR simulations and measurements for the antenna design of mobile devices. These simulated results imply that the location of the SAR hotspot depends completely on the dielectric

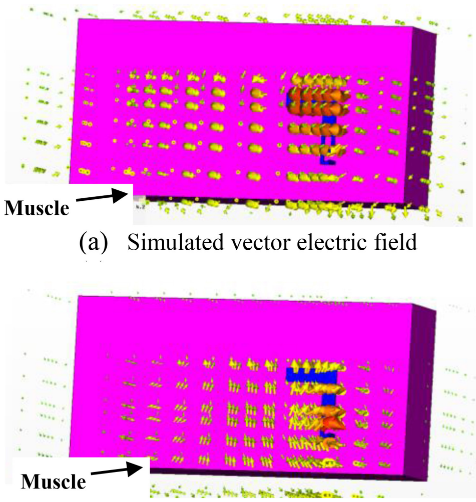

(b) Simulated vector magnetic field

FIGURE 4. Vector fields between the antenna and the muscle tissue.

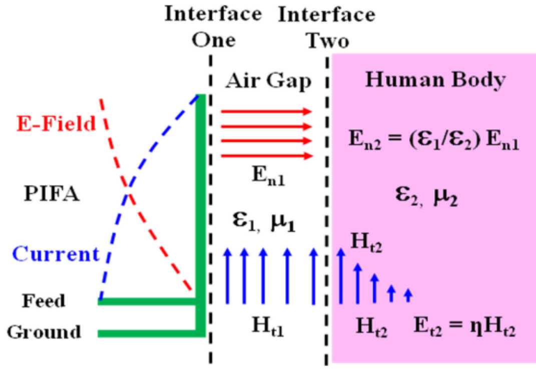

FIGURE 5. Simplified model of PIFA, air gap and human body.

constant value of the block of the loss human tissue. For the human tissue with a very high dielectric constant, such as the human muscle, the SAR hotspot is located at the high electric current (the strong tangential magnetic field) area of the antenna, and for the human tissue with a low dielectric constant, the SAR hotspot is located at the high electric field area of the antenna. A model similar to that shown in Fig. 1 at frequency 860 MHz has also been simulated. The results are very similar to those at the frequency 1800 MHz presented above.

III. ANALYSIS USING BOUNDARY CONDUCTIONS

In this section, we study the unexplained phenomenon outlined above based on electromagnetic boundary conditions. The vector electromagnetic fields in the air gap between the PIFA antenna and the human muscle have been simulated as shown in Fig. 4. As can be observed, the normal component of the vector electric field is much more dominant than the tangential component, whereas the tangential component of the magnetic field is much stronger than the normal component.

The field distribution presented in Fig. 4 could be explained by examining the interfaces of the simulated model. Fig. 5 shows a diagram illustrating a simplified model of the PIFA, the air gap and the human body. The two sides of interface one are air and an antenna radiator, which is usually a good conductor. The boundary conditions of electromagnetic fields at interface one in the air gap region could be approximately considered as the boundary conditions of a perfect conductor, which is given by the following equations:

$$\mathbf{E_{n1}} = \rho_s/\varepsilon_0 \tag{2}$$
$$\mathbf{H_{n1}} = \mathbf{0} \tag{3}$$
$$\mathbf{E_{t1}} = \mathbf{0} \tag{4}$$
$$\mathbf{H_{t1}} = \mathbf{J_s} \tag{5}$$

where the subscript "**n**" and "**t**" denote the normal component and tangential component of the fields, and ρ_s and $\mathbf{J_s}$ are the electric surface charge density and current density at the interface, respectively. The "1" denotes region one, namely the air gap region. As the air gap is electrically a very small region, the electromagnetic field distribution in the air gap is approximately the same as the boundary condition of the perfect conductor described in equation (2)-(5), which indicates that the normal component of the electric field and the tangential component of the magnetic field are much more dominant than the other components. The above analysis is probably a good explanation for the electromagnetic field distribution shown in Fig. 4.

For interface two, as shown in Fig. 5, air and the human body are at the two sides, and the boundary conditions of electromagnetic fields could be approximately considered as the boundary conditions at a dielectric interface though the human body is not an ideal dielectric material. These boundary conditions are given by the following equations:

$$\mathbf{E_{n2}} = (\varepsilon_1/\varepsilon_2)\mathbf{E_{n1}} \tag{6}$$
$$\mathbf{H_{n2}} = (\mu_1/\mu_2)\mathbf{H_{n1}} \tag{7}$$
$$\mathbf{E_{t2}} = \mathbf{E_{t1}} \tag{8}$$
$$\mathbf{H_{t2}} = \mathbf{H_{t1}} \tag{9}$$

where the subscript "**n**" and "**t**" denote the normal component and tangential component of the fields, and ε and μ are the dielectric constant and permeability, respectively. The subscript "1" denotes region one, namely the air gap region, while the subscript "2" denotes region two, namely the human body region. In accordance with equation (6), the attenuation factor of the dominant normal component of the electric field from the air gap to the human body is $\varepsilon_1/\varepsilon_2$, where ε_1 is air dielectric constant and ε_2 the dielectric constant in the human body. It is therefore very difficult for the electric field to penetrate from the air gap into the human body if the human body has a very large dielectric constant. On the other hand, based on equation (7) and (9), both of the components of the magnetic field continue at the interface between the air gap and the human body since permeability of the human body is the same as that of air. This implies that the magnetic field can easily penetrate into the human body from the air gap. Furthermore, as indicated in Fig. 5, in the human body, an electric field is induced by the magnetic field because the propagation wave is a travelling wave in the human body being basically a homogenous and loss material. The strength of the induced electric field is determined by the wave impedance in the human body given by $\eta = \sqrt{(\mu_2/\varepsilon_2)}$. The main reason why the propagation wave in the human body is a travelling wave rather than a standing wave is that there is virtually no reflection wave within the human body, because the electromagnetic wave has been totally absorbed by the high loss human body before it reaches a discontinues boundary.

To summarize the above analysis, the mechanism of electromagnetic absorption by the human body for the usage of mobile devices could be described as follows: when a mobile device is closely placed near the human body, in the air gap between the mobile device's antenna and/or PCB and the human body, the normal component of the electric field and the tangential component of the magnetic field are much more dominant than the other components. The electric field cannot penetrate into the human body because of the high attenuation factor $\varepsilon_1/\varepsilon_2$ if the human body has a very high dielectric constant, whereas the magnetic field could penetrate into the human body freely due to the continuous boundary conditions at the interface. The penetrated magnetic field could induce electric field in the human body because the propagation of electromagnetic field is a travelling wave. The induced electric field is subsequently absorbed by the human body, and the measure of that absorption is defined by Specific Absorption Rate (SAR). Consequently, the hotspot of the SAR is at the location of the maximum magnetic field that corresponds to the maximum electric current area of the antenna. It should be noted that the PIFA antenna shown in Fig. 5 could be replaced by a PCB or any other kind of metallic component in which the electric current is excited by the antenna connecting to the PCB. In such circumstances, the mechanism of electromagnetic absorption by the human body is the same.

IV. SIMULATIONS OF HUMAN PHANTOM HEAD

To further validate the mechanism of electromagnetic absorption by the human body, it is pertinent to examine a more realistic model. Fig. 6 shows the simulated model of a phantom head and hand with a mobile handset at frequency = 1800 MHz. The simulated electric field and loss are illustrated in Fig. 7. As can be seen, there is a clear border between the air gap and the human head. The simulated magnetic fields and loss are depicted in Fig. 8, from which it can be observed that the magnetic field continues at the interface between the human head and the air gap. A similar model at frequency = 850 MHz has also been simulated, and the results are almost identical. These simulated results are in agreement with the mechanism of electromagnetic absorption by the human body outlined in the previous section.

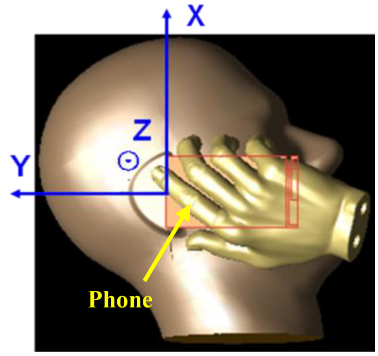

FIGURE 6. Simulated model of a phone beside a phantom head.

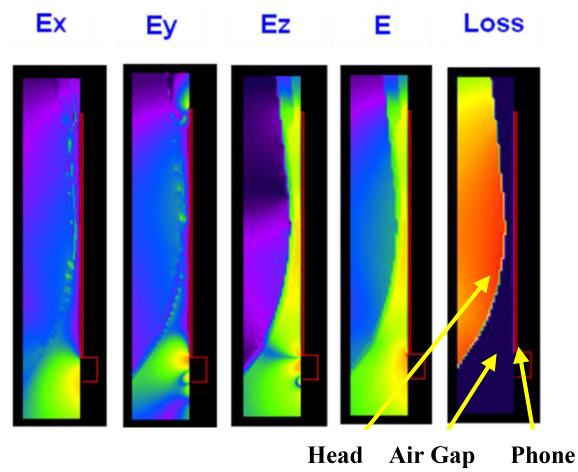

FIGURE 7. Cross section of electric field distribution (Y-O-Z plane).

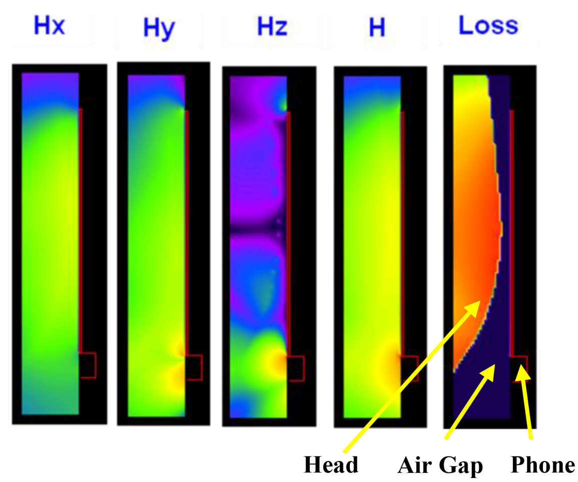

FIGURE 8. Cross section of magnetic field distribution (Y-O-Z plane).

V. CONCLUSION

The mechanism of electromagnetic absorption by the human body has been comprehensively studied using the boundary conditions and simulations of electromagnetic fields. A "contradiction" that has puzzled many researchers and engineers for many years has been clearly explained. It is expected that the presented analytical methodology and conclusions could have significant impact on the research of SAR reduction and antenna efficiency improvement when a hand-held or wearable mobile device is closely placed to the human body.

ACKNOWLEDGMENT

The author wishes to thank L. N. Chen, who was previously with Huawei Technologies, for her help in the simulation.

REFERENCES

[1] P. Bahramzy, S. Svendsen, O. Jagielski, and G. F. Pedersen, "SAR study of mobile phones as a function of antenna Q," *IEEE Trans. Antennas Propag.*, vol. 63, no. 9, pp. 4139–4147, Sep. 2015.

[2] K. Han *et al.*, "Magneto-dielectric nanocomposite for antenna miniaturization and SAR reduction," *IEEE Antennas Wireless Propag. Lett.*, vol. 15, pp. 72–75, 2016.

[3] J. Trajkovikj and A. K. Skrivervik, "Diminishing SAR for wearable UHF antennas," *IEEE Antennas Wireless Propag. Lett.*, vol. 14, pp. 1530–1533, 2015.

[4] S. I. Kwak, D. U. Sim, J. H. Kwon, and Y. J. Yoon, "Design of PIFA with metamaterials for body-SAR reduction in wearable applications," *IEEE Trans. Electromagn. Compat.*, vol. 59, no. 1, pp. 297–300, Feb. 2017.

[5] H. Li, A. Tsiaras, and B. K. Lau, "Analysis and estimation of MIMO-SAR for multi-antenna mobile handsets," *IEEE Trans. Antennas Propag.*, vol. 65, no. 3, pp. 1522–1527, Mar. 2017.

[6] D. T. Le, L. Hamada, S. Watanabe, and T. Onishi, "A fast estimation technique for evaluating the specific absorption rate of multiple-antenna transmitting devices," *IEEE Trans. Antennas Propag.*, vol. 65, no. 4, pp. 1947–1957, Apr. 2017.

[7] N. Kuster and Q. Balzano, "Energy absorption mechanism by biological bodies in the near field of dipole antennas above 300 MHz," *IEEE Trans. Veh. Technol.*, vol. 41, no. 1, pp. 17–23, Feb. 1992.

[8] H.-R. Chuang, "Numerical computation of fat layer effects on microwave near-field radiation to the abdomen of a full-scale human body model," *IEEE Trans. Microw. Theory Techn.*, vol. 45, no. 1, pp. 118–125, Jan. 1997.

HANYANG WANG (Senior Member, IEEE) received the Ph.D. degree from Heriot-Watt University, Edinburgh, U.K., in 1995.

From 1986 to 1991, he served as a Lecturer and an Associate Professor with Shandong University, Jinan, China. From 1995 to 1999, he was a Postdoctoral Research Fellow with the University of Birmingham, Birmingham, U.K., and the University of Essex, Colchester, U.K. From 1999 to 2000, he was with Vector Fields Ltd., Oxford, U.K., as a software development and microwave and antenna engineering consultant engineer. In 2001, he joined Nokia U.K. Ltd., Farnborough, U.K., where he had been a Mobile Antenna Specialist for 11 years. He joined Huawei after leaving Nokia, and he is currently the Chief Mobile Antenna Expert and the Head of the Mobile Antenna Technology Division, Huawei Technologies. He leads a large group of antenna experts and engineers and takes the full leadership and responsibility in the research and development of antenna technologies to guarantee the market success of all Huawei's mobile terminal products ranging from smartphones, laptops, tablets, MiFi, data cards, smart watches, BT headsets, routers, IoT, smart screens, CPE, VR, and vehicles. He is also an Adjunct Professor with Nanjing University, Nanjing, China, and Sichuan University, Chengdu, China. He holds over 40 granted U.S./EU/JP/CN patents, including 26 U.S. patents, and has over 40 patent applications in pending. His current research interests include small, wideband and multiband antennas for mobile terminals, MIMO antennas and antenna arrays for 5G sub-6 GHz, and 5G millimetre-wave mobile communications. He has authored over 100 papers on these topics. He received the Nokia Inventor of the Year award in 2005, the Nokia Excellence Award in 2011, the Huawei Individual Gold Medal Award in 2012, and the Huawei Team Gold Medal Award in 2013 and 2014. His patent was ranked number one among 2015 Huawei Top Ten Patent Awards. He has been an Associate Editor of IEEE ANTENNAS AND WIRELESS PROPAGATION LETTERS since January 2015. He is a fellow of Huawei and IET.